

# Thermonuclear explosions of Chandrasekhar-mass C+O white dwarfs

M. Reinecke<sup>1</sup>, W. Hillebrandt<sup>1</sup>, and J.C. Niemeyer<sup>2</sup>

<sup>1</sup> Max-Planck-Institut für Astrophysik, Karl-Schwarzschild-Strasse 1, D-85740 Garching, Germany

<sup>2</sup> LASR, Enrico Fermi Institute, University of Chicago, Chicago, IL 60637, USA

Received 20 November 1998 / Accepted 19 April 1999

**Abstract.** First results of simulations are presented which compute the dynamical evolution of a Chandrasekhar-mass white dwarf, consisting of equal amounts of carbon and oxygen, from the onset of violent thermonuclear burning, by means of a new two-dimensional numerical code. Since in the interior of such a massive white dwarf nuclear burning progresses on microscopic scales as a sharp discontinuity, a so-called flamelet, which cannot be resolved by any numerical scheme, and since on macroscopic scales the burning front propagates due to turbulence, we make an attempt to model both effects explicitly in the framework of a finite-volume hydrodynamics code. Turbulence is included by a sub-grid model, following the spirit of large eddy simulations, and the well-localized burning front is treated by means of a level set, which allows us to compute the geometrical structure of the front more accurately than with previous methods. The only free parameters of our simulations are the location and the amount of nuclear fuel that is ignited as an initial perturbation. We find that models in which explosive carbon burning is ignited at the center remain bound by the time the front reaches low densities, where we stopped the computations because our description of combustion is no longer applicable. In contrast, off-center ignition models give rise to explosions which, however, are still too weak for typical Type Ia supernovae. Possible reasons for this rather disappointing result are discussed.

**Key words:** hydrodynamics – nuclear reactions, nucleosynthesis, abundances – turbulence – methods: numerical – stars: supernovae: general

## 1. Introduction

Despite the fact that considerable attention has recently been devoted to so-called sub-Chandrasekhar mass models (see, e.g., Iben & Tutukov 1991; Woosley & Weaver 1994; Livne 1996), the most popular progenitor model for at least some Type Ia supernovae is a massive white dwarf, consisting of carbon and oxygen, which approaches the Chandrasekhar mass,  $M_{\text{Ch}} \simeq 1.39 M_{\odot}$ , by a yet unknown mechanism, presumably

accretion from a companion star, and is disrupted by a thermonuclear explosion (see, e.g., Woosley 1990 for a review). Arguments in favor of this hypothesis include the ability of these models to fit the observed spectra and light curves, in particular in versions that propagate the burning front mostly in form of a sub-sonic deflagration wave.

However, not only is the evolution of massive white dwarfs to explosion very uncertain, leaving room for some diversity in the allowed set of initial conditions (such as the temperature profile at ignition), but also the physics of thermonuclear burning in degenerate matter is complex and not well understood. The generally accepted scenario is that explosive carbon burning is ignited either at the center of the star or off-center in a couple of ignition spots, depending on the details of the previous evolution. For example, URCA-neutrino emission affects the temperature distribution as well as non-steady convection during the slow carbon burning phase prior to the explosion, and both effects are usually not treated in Type Ia models. After ignition, the flame is thought to propagate through the star as a sub-sonic deflagration wave which may or may not change into a detonation at low densities (around  $10^7 \text{g/cm}^3$ ). Numerical models with parameterized velocity of the burning front have been very successful, the prototype being the W7 model of Nomoto et al. (1984). However, these models do not solve the problem because attempts to determine the effective flame velocity from direct numerical simulations failed and gave velocities far too low for successful explosions (Livne, 1993; Khokhlov, 1995; Arnett & Livne, 1994). This has led to some speculations about ways to change the deflagration into a supersonic detonation (Khokhlov, 1991a,b,c).

Here, as well as in several previous papers (Niemeyer & Hillebrandt, 1995; Niemeyer et al., 1996; Niemeyer & Woosley, 1997), we aim at a better understanding and a more accurate numerical treatment of thermonuclear deflagration waves in degenerate C+O white dwarfs, hoping to resolve the difficulties of this class of supernova models. In order to clarify the problem we shall first discuss in Sect. 2 the basic physics of deflagration fronts in the flamelet regime as well as attempts to model them by numerical simulations. In Sect. 3 we present a brief description of our new numerical method. The results of a series of computations are given and discussed in Sect. 4 and, finally, Sect. 5 is devoted to a summary and outlook on future work.

---

Send offprint requests to: M. Reinecke  
(martin@mpa-garching.mpg.de)

## 2. A model for turbulent combustion in the flamelet regime

Nuclear burning in the degenerate matter of a dense C+O white dwarf, once ignited, is believed to propagate on microscopic scales as a conductive flame, wrinkled and stretched by local turbulence, but with essentially the laminar velocity. At high densities near the center of a Chandrasekhar-mass white dwarf the typical length scales for the width of the flame are a fraction of a millimeter. However, this is not the most relevant length scale. Due to the very high Reynolds numbers, which are of the order of  $10^{14}$  on typical macroscopic scales of  $10^7$  cm, macroscopic flows are highly turbulent and interact with the flame, in principle down to the Kolmogorov scale of  $10^{-3}$  cm. This means that all kinds of hydrodynamic instabilities feed energy into a turbulent cascade, including the buoyancy-driven Rayleigh-Taylor instability and the shear-driven Kelvin-Helmholtz instability (see, e.g., Niemeyer & Hillebrandt 1995 and Hillebrandt & Niemeyer 1997). Consequently, the picture that emerges is more that of a “flame brush” spread over the entire turbulent regime rather than a wrinkled flame surface. For such a flame brush, the relevant minimum length scale is the so-called Gibson scale, defined as the lower bound for the curvature radius of flame wrinkles caused by turbulent stress. Thus, if the thermal diffusion scale is much smaller than the Gibson scale (which is the case for the physical conditions of interest here) small segments of the flame surface are unaffected by large scale turbulence and behave as unperturbed laminar flames (“flamelets”). On the other hand side, since the Gibson scale is, at high densities, several orders of magnitude smaller than the integral scale set by the Rayleigh-Taylor eddies and many orders of magnitude larger than the thermal diffusion scale, both transport and burning times are determined by the eddy turnover times, and the effective velocity of the burning front is independent of the laminar burning velocity. This general picture has indeed been verified by laboratory combustion experiments (see, e.g., Abdel-Gayed et al. 1987).

Niemeyer (1995) and Niemeyer & Hillebrandt (1995) have presented a numerical realization of this general concept. Their basic assumption was that wherever one finds turbulence this turbulence is fully developed and homogeneous, i.e. the turbulent velocity fluctuations on a length scale  $l$  are given by the Kolmogorov law

$$v(l) = v(L) \left( \frac{l}{L} \right)^{1/3}, \quad (1)$$

where  $L$  is the integral scale, assumed to be equal to the Rayleigh-Taylor scale. Following the ideas outlined above, one can also assume that the thickness of the turbulent flame brush on the scale  $l$  is of the order of  $l$  itself. With these two assumptions and the definition of the Gibson scale one finds for  $l_{\text{gibs}} \lesssim l \lesssim L \simeq \lambda_{\text{RT}}$  that

$$v(l) \simeq u_t(l) \simeq u_t(l_{\text{gibs}}) \left( \frac{l}{l_{\text{gibs}}} \right)^{1/3} \quad (2)$$

and

$$d_t(l) \simeq l, \quad (3)$$

where  $v(l_{\text{gibs}}) = u_{\text{lam}}$  defines  $l_{\text{gibs}}$ ,  $u_{\text{lam}}$  is the laminar burning speed and  $u_t(l)$  is the turbulent flame velocity on the scale  $l$ .

In a second step this model of turbulent combustion is coupled to a finite volume hydro scheme such as the PPM-code PROMETHEUS (Fryxell et al., 1989). Since in every finite volume scheme scales smaller than the grid size cannot be resolved, we express  $l_{\text{gibs}}$  in terms of the grid size  $\Delta$ , the (unresolved) turbulent kinetic energy  $q$ , and the laminar burning velocity:

$$l_{\text{gibs}} = \Delta \left( \frac{u_t^2}{2q} \right)^{3/2}. \quad (4)$$

Here  $q$  is determined from a sub-grid model (Clement, 1993; Niemeyer & Hillebrandt, 1995) and, finally, the effective turbulent velocity of the flame brush on scale  $\Delta$  is given by

$$u_t(\Delta) = \max(u_{\text{lam}}, v(\Delta), v_{\text{RT}}), \quad (5)$$

with  $v(\Delta) = \sqrt{2q}$  and  $v_{\text{RT}} \propto \sqrt{g\Delta}$ , where  $g$  is the local gravitational acceleration.

The numerical scheme outlined so far has been applied to two-dimensional simulations of explosive C-burning in  $M_{\text{Ch}}$ -mass C+O white dwarfs by Niemeyer & Hillebrandt (1995) and Niemeyer et al. (1996) for a variety of initial conditions. They found that, with the exception of a model that was ignited off-center in a single small blob, all models were unbound at the end of the computations, and between  $0.59 M_{\odot}$  (for central ignition) and  $0.65 M_{\odot}$  of matter had been burnt, which would guarantee an observable, although weak, Type Ia supernova, but certainly not an average one, in particular because the expansion velocities were too low.

There are two possible interpretations of these results. Either they show that the “normal” Type Ia supernova is *not* the result of the explosion of a  $M_{\text{Ch}}$ -mass C+O white dwarf, caused by a deflagration wave, or the modeling of thermonuclear combustion as outlined so far is still insufficient. In this paper we investigate the second possibility and, in particular, present results obtained by means of an improved numerical scheme. The main aim is to cure a problem that is common to all finite volume schemes, namely that, although discontinuities are captured automatically, they are smeared artificially over several grid zones. In many applications this broadening of discontinuities might not be a big problem but for modeling turbulent combustion one cannot be satisfied.

The reasons for this are simple. First, as we discussed already, it is important to reproduce the geometry of the flame front as accurately as possible, because its effective surface area also determines the rate of fuel consumption. If we think of the flame in terms of a surface of a given fractal dimension the minimum scale determines essentially its effective velocity. Therefore it is important to resolve the small scales as accurately as possible. Secondly, since nuclear reactions are very sensitive to temperature and their rates depend on a very high power of  $T$ , mixing fuel and ashes numerically in certain mesh points on both sides of the front and smearing out the temperature gradient there will lead to huge errors in the (local) energy generation rates. Therefore, if in a code one wants to follow the nuclear transmutations explicitly one is forced to guarantee that

temperature jumps due to fast reactions are tracked with high precision.

A possible way to reach both goals is to track the front by means of a level set function and to reconstruct the thermodynamical quantities in front and behind the the discontinuity from conservation laws. This approach has been utilized successfully for simulations of terrestrial hydrogen combustion by Smiljanovski et al. (1997) and was reformulated and coded for the application to thermonuclear combustion in C+O white dwarfs by Reinecke et al. (1998). Here we apply a somewhat simplified version of this code, i.e. we still assume, as in Niemeyer & Hillebrandt (1995) and Niemeyer et al. (1996), that the matter of the white dwarf is defined by two states, fuel and ashes, respectively, and that the transition from fuel to ashes is given by the instantaneous liberation of a certain amount of energy  $q$  once the material crosses the flame front. Thus the front-tracking by the level-set function can be interpreted as a kind of passive advection without reconstruction. Nonetheless, in contrast to common front capturing schemes, our code is able to resolve complex structures of the flame on small scales.

### 3. The numerical method

The numerical code applied in this work is again based on the PPM code PROMETHEUS (Fryxell et al., 1989) combined with a sub-grid model for unresolved turbulence, as was outlined in Sect. 2 (see also Niemeyer & Hillebrandt (1995)). This includes that the propagation velocity of the burning front is obtained from the local turbulent kinetic energy as given by Eq. (5).

As a model for the flame, we use the so-called level set approach first described by Osher & Sethian (1988). The key concept of this model is to associate the flame front  $\Gamma(t)$  with the zero level set of a scalar function  $G(\mathbf{r}, t)$ :

$$\Gamma(t) := \{\mathbf{r} \mid G(\mathbf{r}, t) = 0\} \quad \forall t \quad (6)$$

This condition does not fully determine  $G$ . For numerical reasons it is appropriate to postulate also that  $G$  be positive in the burnt regions and negative before the front and that

$$|\nabla G| \equiv 1, \quad (7)$$

which means that  $G$  is a signed distance function.

This flame description is well suited for the combustion in Type Ia supernovae for a variety of reasons:

- The front is modeled as a discontinuity between fuel and ashes; this is an excellent approximation, if one compares the flame width and the typical cell size. A piecewise linear representation of the front is easy to obtain.
- Complex topological situations, like the breaking of the burnt area into several disconnected regions, re-merging and highly convoluted front geometries are handled without problems.
- The approach can be used for an arbitrary number of simulated dimensions. An extension to three-dimensional problems is straightforward.

$G(\mathbf{r}, 0)$  is defined by the initial conditions. During the simulation, the front propagates with the velocity

$$\mathbf{v}_{\text{flame}} = \mathbf{v}_u + u_t \mathbf{n} \quad (8)$$

with respect to the underlying grid, where  $\mathbf{v}_u$  represents the velocity of the unburnt material and  $\mathbf{n}$  is the front normal pointing towards the unburnt material. This leads to the following expression for the temporal evolution of  $G$  in the vicinity of the front:

$$\frac{\partial G}{\partial t} = -\mathbf{v}_{\text{flame}} \nabla G = (\mathbf{v}_u \mathbf{n} + u_t) |\nabla G| \quad (9)$$

To preserve the distance-function property, an additional re-initialization step is necessary; see Reinecke et al. (1998) and Smiljanovski et al. (1997) for a detailed discussion.

The level set propagation according to Eq. 9 requires the knowledge of the velocity of the unburnt material  $\mathbf{v}_u$  at the front. Although this value can, in principle, be calculated in the cells cut by the front (Smiljanovski et al., 1997), the extreme thermodynamical properties of the degenerate white dwarf material make this reconstruction very difficult.

Fortunately, under the conditions typical for Type Ia supernovae, the velocity jump is quite small compared to the burning velocity, so that  $\mathbf{v}_u$  can be approximated by the average flow velocity with only small error. In this case, the hydrodynamical advection of  $G$  can be written in conservation form:

$$\int_V \frac{\partial(\rho G)}{\partial t} d^3r + \oint_{\partial V} \mathbf{v}_F \rho G d\mathbf{f} = 0 \quad (10)$$

Therefore it is possible to treat the advection of the front caused by the fluid movement with the Godunov method built into PROMETHEUS.

The propagation of the front, the species conversion and the energy release due to burning is done in an additional subroutine. In this step we apply

$$G' = G + \Delta t u_t \sqrt{D_x^2 + D_y^2}, \quad (11)$$

where  $D_x$  and  $D_y$  represent discrete gradients. Next, the burnt volume fraction of all cells cut by the front are calculated, and the chemical composition and energy of these cells is adjusted.

### 4. Results and discussion

We have carried out numerical simulations in cylindrical rather than in spherical coordinates, mainly because it is much simpler to implement the level set on a Cartesian  $(r, z)$  grid. Moreover, we save computer time since we avoid very small CFL time-steps which result in spherical coordinates near the center of the star if one wants to have good angular resolution.

The grid we used maps the white dwarf onto  $256 \times 256$  mesh points, equally spaced for the innermost  $226 \times 226$  zones by  $\Delta = 1.5 \cdot 10^6$  cm, but increasing by 10% from zone to zone in the outer parts. The white dwarf, constructed in hydrostatic equilibrium for a realistic equation of state, has a central density of  $2.9 \cdot 10^9$  g/cm<sup>3</sup>, a radius of  $1.5 \cdot 10^8$  cm, and a mass of  $2.8 \cdot 10^{33}$  g,

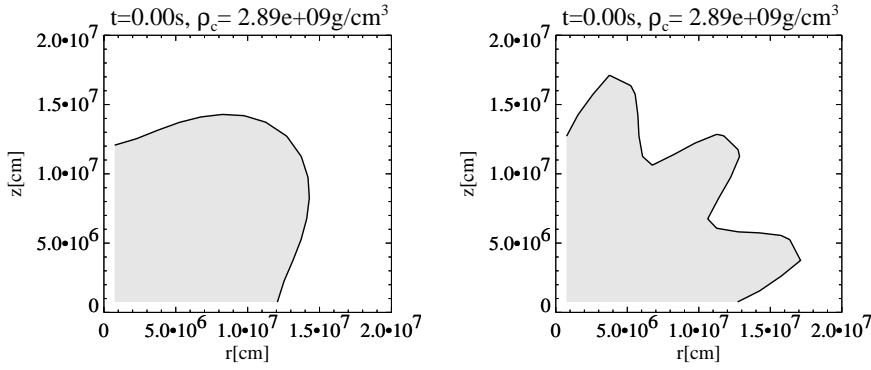


**Fig. 1.** Initial front geometry for the centrally ignited models C1 and C3.

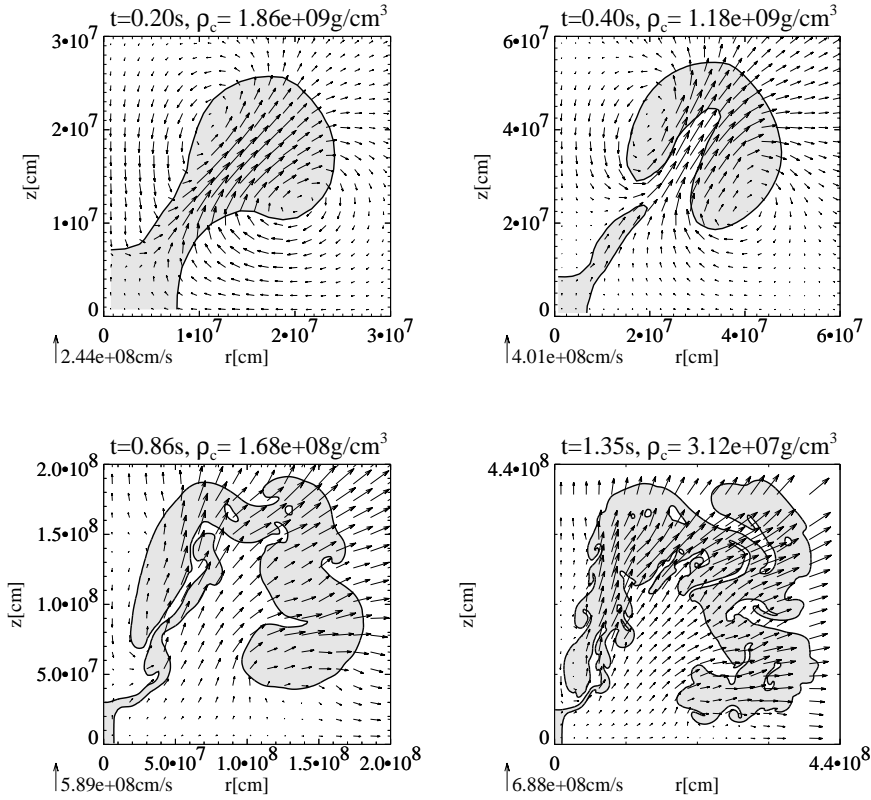


**Fig. 2.** Temporal evolution of front geometry and velocity distribution for model C1. The unequal spacing of the velocity arrows in the last snapshot results from the non-equidistant grid points. Note that all scales change from snapshot to snapshot.

identical to the one used by Niemeyer & Hillebrandt (1995). The initial mass fractions of C and O are chosen to be equal, and the total binding energy turns out to be  $5.4 \cdot 10^{50}$  erg. Finally, in order to solve for the sub-grid turbulent kinetic energy, we have to specify its initial values on the grid and we assume a constant small value of  $q=10^{12}$  erg/g, again in agreement with Niemeyer & Hillebrandt (1995). This latter assumption is justified because after a very short time  $q$  adjusts to the local turbulence, independent of its initial value. At low densities ( $\rho \leq 10^7$  g/cm<sup>3</sup>), the burning velocity of the front is set equal to zero because the flame enters the distributed regime and our physical model is no longer valid. However, since in reality significant amounts of mass may be burned at lower densities, the energy release obtained from our simulations is a lower limit only. On the other hand, it is difficult to estimate the error due to this simplification, mainly because the physics in the distributed regime of burning is not yet understood. It may happen that the flame just “stalls”,

in which case our numerical description would be appropriate. In the other extreme, even a deflagration-to-detonation transition (DDT) is not excluded which would change the energetics considerably.

#### 4.1. Centrally ignited models

In this set of simulations we start the computations assuming that the inner  $1.5 \cdot 10^7$  cm, corresponding to a mass of about  $0.02M_{\odot}$ , are burnt. In addition, a sinusoidal perturbation is superimposed producing one “finger” (model C1) or three fingers (model C3), respectively, as seeds for the Rayleigh-Taylor instability (see Fig. 1).

Fig. 2 shows a sequence of snapshots of the front geometry and the velocity field for model C1 (note that all scales change from snapshot to snapshot). The burnt matter is shaded and the front, given by the level set function, is plotted as a solid

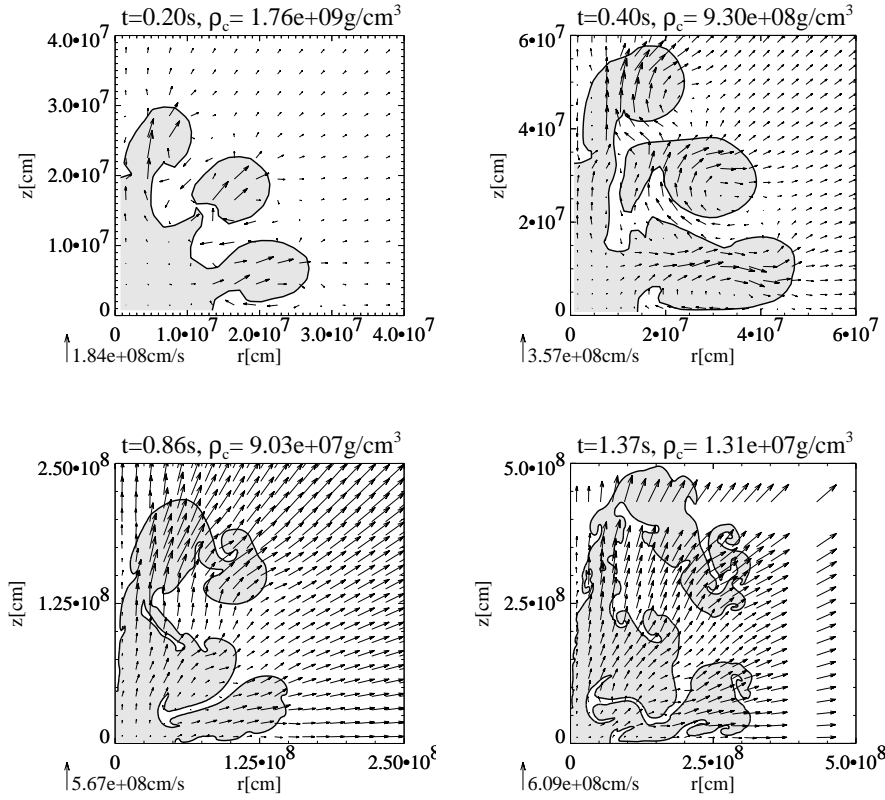


**Fig. 3.** Temporal evolution of front geometry and velocity distribution for model C3.

line. The evolution follows essentially one's intuition. First the "finger" grows into a typical Rayleigh-Taylor structure, mainly in radial direction, giving rise to two vortices on both sides of the Rayleigh-Taylor head. There, the turbulence intensity increases and nuclear burning is accelerated, leading, in turn, to still faster motions. For a while, a burning blob even disconnects from the much slower burnt matter near the center of the star. In part, this is due to our symmetry assumptions which force us to use reflecting boundary conditions on both coordinate axes, but it also shows that our code can handle multiply connected fronts.

After about 1s most of the matter of the white dwarf is expanding and roughly  $0.3M_{\odot}$  have been burnt into Ni, too little to unbind the star. The structure of the burnt region becomes very complex. Kelvin-Helmholtz whirls can be seen at the interfaces between rising hot matter and unburnt more slowly expanding fuel. Once the central density has dropped to  $3 \cdot 10^7 \text{g/cm}^3$  we stopped the calculations for the reason which was explained earlier. The amount of Ni produced then is nearly  $0.33M_{\odot}$ . The obvious asymmetries in the flow patterns at late times are again a consequence of the imposed symmetry conditions: Convective eddies are not bubbles but axi-symmetric rings, and while for an equidistant grid the cell volume does not increase in  $z$ -direction, it does so in radial direction proportional to  $r$  because of the axi-symmetry.

Fig. 3 shows snapshots of model C3 where we started the computations with three "fingers" rather than one. The changes again are not unexpected. Due to the more complex initial perturbation burning propagates faster in the beginning, mainly because the effective surface of now three Rayleigh-Taylor bub-

bles is bigger. The net effect, however, is that already after about 0.6s the white dwarf expands and cools, and, in the end, the total amount of Ni produced is only marginally higher, by about 10%, as in model C1, but also this model remains weakly bound.

#### 4.2. Off-center ignition models

In two more simulations we follow the work of Niemeyer et al. (1996) and ignite the carbon and oxygen fuel off-center, first in one blob and then in five ones (models B1 and B5; see Fig. 4 for the initial configurations). Since these blobs can rise freely, not connected to the center by a symmetry condition, we expect that they move faster, thereby generating more turbulence and, consequently, also more rapid burning. Figs. 5 and 6 demonstrate that this expectation is indeed fulfilled by the simulations. In models B1 and B5, after 0.61s, peak velocities are typically higher than those of models C1 and C3 by up to 50%. Because fuel is consumed very rapidly in B1 and B5 also the expansion sets in earlier. However, this does not extinguish the burning in the case of model B5. In contrast, because of the large surface of the various burning blobs fuel consumption progresses so fast that this model is unbound already after 0.5s, and continues to burn until the amount of Ni is  $0.34M_{\odot}$ . Therefore, in our computations this model is the only one which gives rise to an observable supernova explosion. Model B1, on the other hand side, ends also unbound, but its total energy at the end of the computations is close to zero.

A final remark concerns numerical effects which are obviously present in our simulations and which may affect the

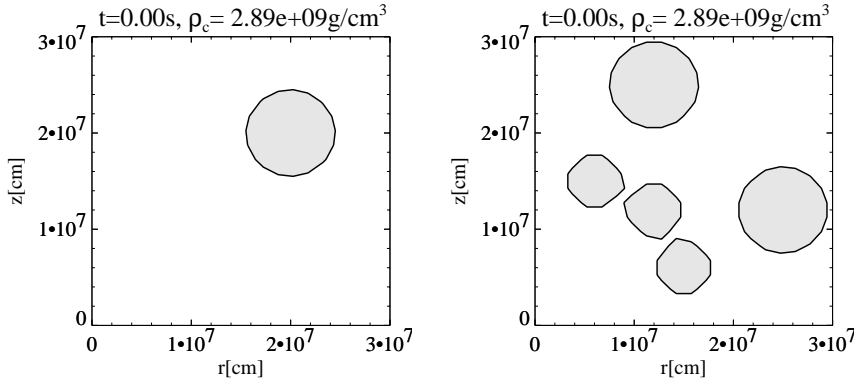


**Fig. 4.** Initial front geometry for the off-center ignited models B1 and B5.

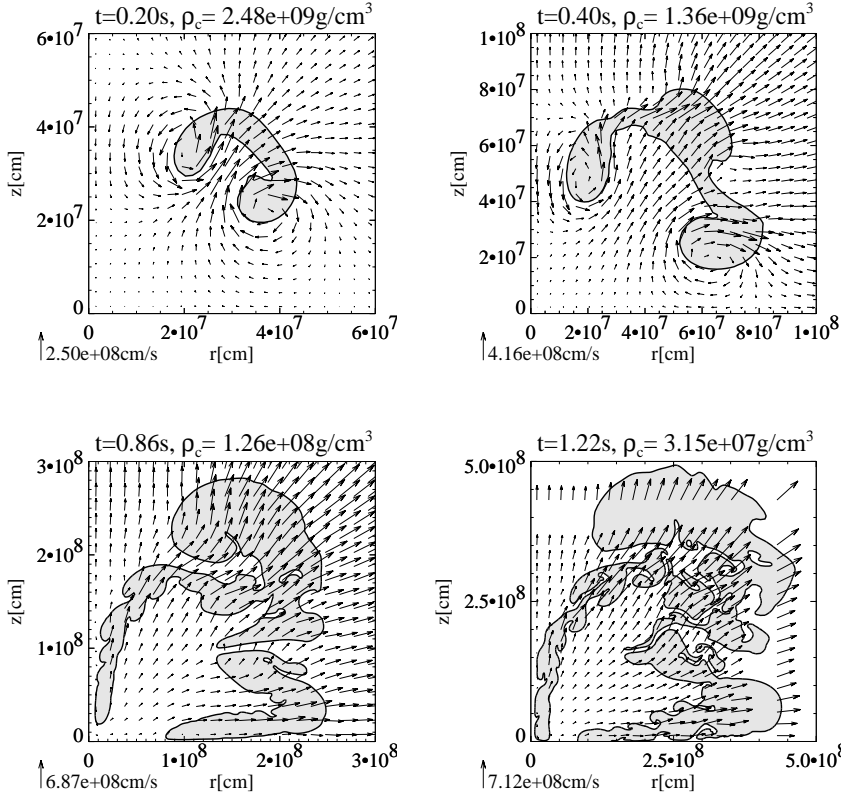


**Fig. 5.** Temporal evolution of front geometry and velocity distribution for model B1.

outcome. First, as was stated before, in three dimensions without artificial symmetry assumptions Rayleigh-Taylor eddies will move faster. Moreover, a multiple of rising blobs has a higher surface area than our Rayleigh-Taylor “rings”. Both effects will increase the rate of fuel consumption and, therefore, will work in favor of more violent explosions. Moreover, due to finite numerical resolution, the minimum scale of eddies shown in the previous figures is certainly too large. For example, whenever blobs disconnect from each other, this is because burning strings in between them are not resolved. This, in turn means that our code still underestimates the total rate of nuclear burning. Of course, we hope that to a certain extent the subgrid model for the unresolved turbulent scales takes care of these effects. However, since we do not resolve the smallest RT-unstable wavelengths the assumption of a Kolmogorov-spectrum on sub-grid scales may not be justified and, even more important, we may not have

enough spatial resolution to reach the turbulent regime. In principle, this hypothesis could be tested by increasing the resolution significantly, making the simulations very expensive, and first results of simulations with  $\Delta = 5 \cdot 10^5$  cm give (after  $t \approx 0.6$ s) indeed a considerably higher energy production rate than the models discussed above, indicating that the calculations are not fully converged. It appears to be unlikely, however, that going to higher numerical resolution will change our main conclusions.

A numerical comparison of all four models at the end of the simulation is given in Table 1.

#### 4.3. A comparison with previous works

The results outlined so far should be compared to those of Niemeyer (1995), Niemeyer & Hillebrandt (1995) and Niemeyer et al. (1996), because the main motivation behind

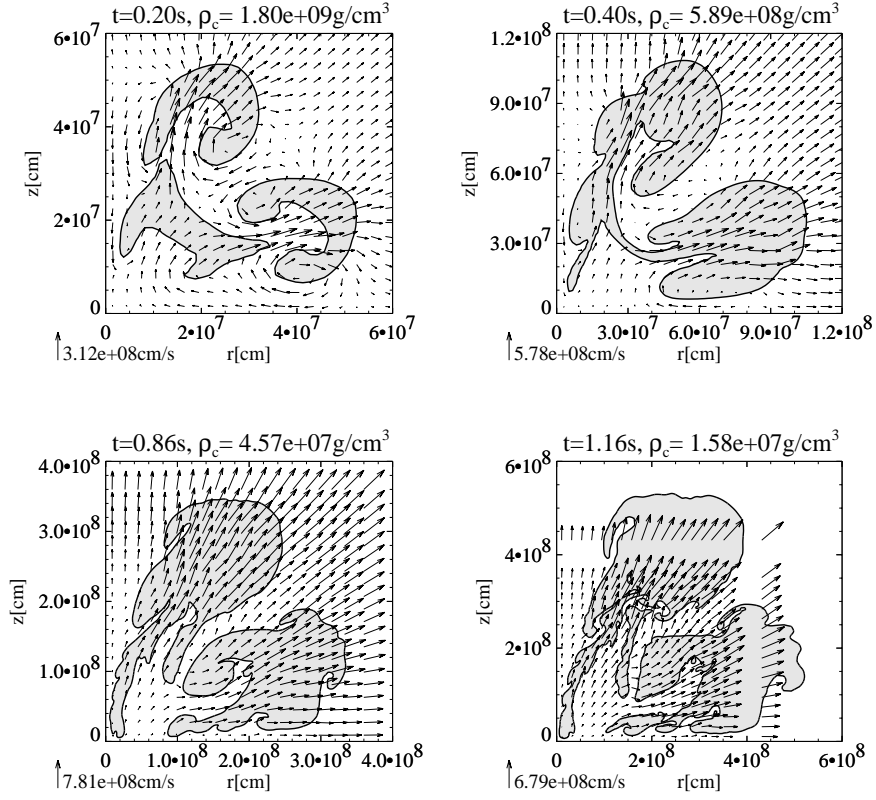


**Fig. 6.** Temporal evolution of front geometry and velocity distribution for model B5.

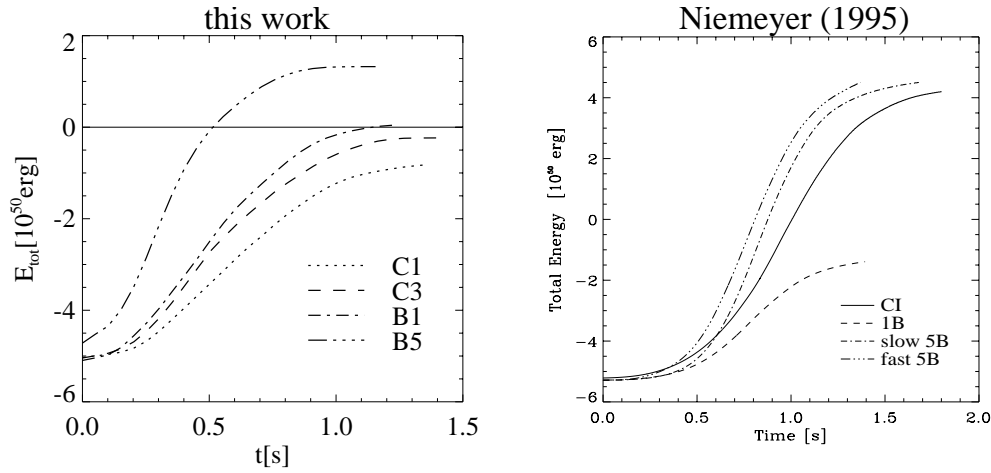


**Fig. 7.** Temporal evolution of the total energy

**Table 1.** Comparison of integral quantities at the end of the four simulations. The numbers given are only approximate because of some mass-loss from the computational grid at late stages.

	C1	C3	B1	B5
Elapsed time [s]	1.35	1.43	1.22	1.16
Total mass of $^{56}\text{Ni}$ [ $M_{\odot}$ ]	0.23	0.26	0.27	0.34
Total energy [ $10^{50}$ erg]	-0.82	-0.23	0.04	1.32
Kinetic energy [ $10^{50}$ erg]	1.95	2.00	2.55	3.11

our present work was to improve their numerical treatment of a turbulent burning front in the flamelet regime, hoping that such improvements would change their weak explosions into more violent ones. Now the contrary appears to be true.

In order to make the comparison more quantitative we plot in Figs. 7 through 9 the total energy, the nuclear energy generation rate, and the turbulent sub-grid energy as functions of time for our models and for some models from the previous papers. Since with the exception of the front-tracking scheme of the present computations both codes are identical, simulations with similar initial conditions allow us to compare the effects caused by the flame-propagation model. In this respect, our model B1 and the model 1B of Niemeyer (1995), as well as B5 and his “slow 5B” are similar. The same holds for our model C3 and Niemeyer’s CI, with the difference that the perturbation wavelength in our simulation had to be larger due to limited angular resolution near the center of the star.

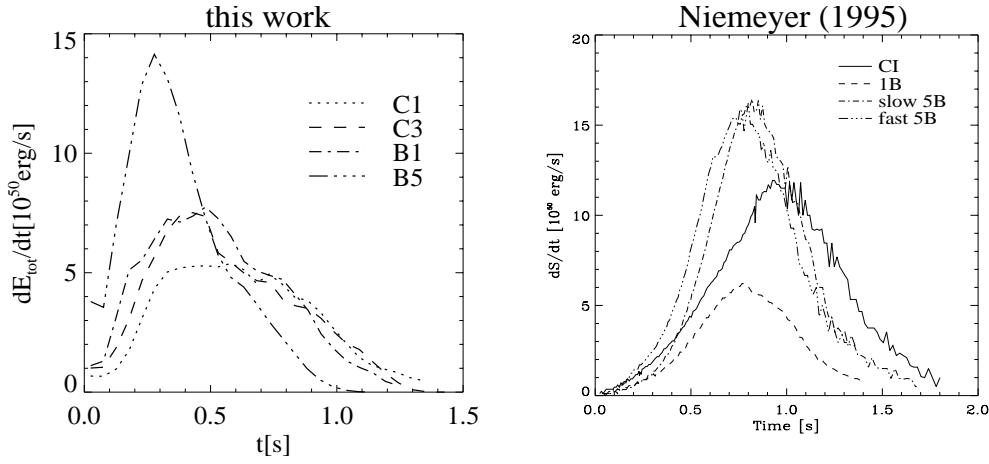


**Fig. 8.** Temporal evolution of the energy production by combustion

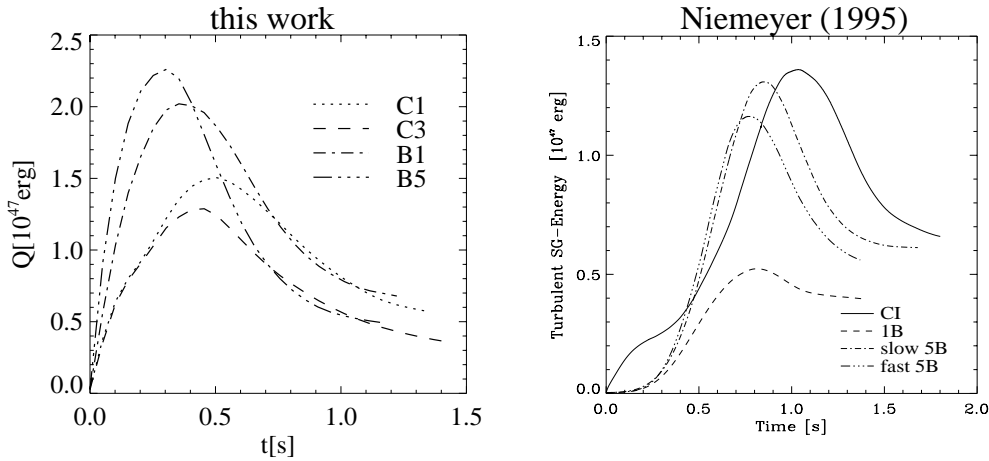


**Fig. 9.** Temporal evolution of the turbulent sub-grid energy

The first major difference seen in Fig. 7 is that, in contrast to our expectations, the code with front-tracking in general produces *less* energy from nuclear burning than the other one. (Note that the energies plotted include already the energy liberated in the initial perturbation. Therefore the curves do not start from the same value at time  $t=0$ s.) But a closer look at Figs. 8 and 9 reveals the reason. Fig. 8 gives the energy generation rate for the various models. In those models with front-tracking the energy generation rate rises more rapidly in the beginning, caused by the rapid increase of the turbulent sub-grid energy (see Fig. 9), in contrast to the models without front-tracking. This, in fact, is in agreement with ones expectations because the tracked front has more structure and, therefore, a larger surface area. However, already after 0.5s the total energy released by nuclear burning in all our present models is high enough to lead to an overall expansion of the white dwarf, as was discussed in the previous subsections. Consequently, the sub-grid energy drops again and so does the nuclear energy generation rate. So in total less energy is produced in comparison to the models without tracking, which reach their peak values of both the energy generation and the sub-grid energy about a factor of two later and, therefore, expand later. An exception is our model B5. Here the energy generation rate rises so fast that the star is already unbound at the time when bulk expansion sets in.

In addition to the higher sub-grid energy production during the early stages of the simulations, we observe that most of the turbulence is generated in a very thin region around the flame, resulting in extremely high turbulence intensities near the front and a further increase in the burning speed (Fig. 10). This is caused by the fact that the transition between the rising bubbles of hot, light ashes and the dense, cold fuel is quite thin ( $\approx 2\Delta$ ), which leads to a well-localized shear flow and turbulent energy generation, as one would expect in reality. In Niemeyer's simulations, in contrast, the transition was smeared out over several cells because of the employed reactive-diffusive flame model; consequently, the turbulent flame propagation speed was underestimated.

## 5. Summary and conclusions

In the present paper we have presented first results obtained by applying a new numerical technique to thermonuclear explosions of Chandrasekhar-mass C+O white dwarfs. Our code differs from those used previously in the astrophysics literature in that it follows the propagation of the burning front explicitly by means of a level set function. Our approach has the advantage that numerical diffusion of the front is largely avoided and that the structure of burning regions is resolved down to a few grid zones, which is an important issue in numerical simulations of

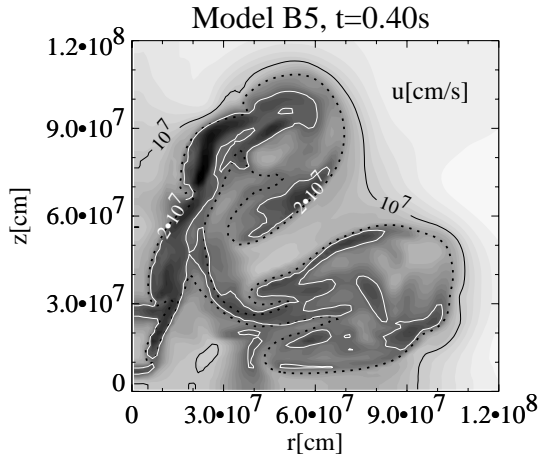


**Fig. 10.** Distribution of the turbulent velocity fluctuations (Model B5, after 0.4s)

combustion. Moreover, in principle, an extension of the code is possible, making use of the fact that the thermodynamic properties in mixed cells can be reconstructed from the conservation laws of mass, energy, and momentum, if the burning velocity of the front is known. Such a code could also be applied to the Type Ia supernova problem and would, for the first time, allow to include individual nuclear reactions in a meaningful way, and we are presently working on this extension.

Since our aim was to demonstrate that deflagrations in  $M_{\text{Ch}}$  white dwarfs can lead to explosions which have the properties of some (if not of typical) Type Ia supernovae, the outcome so far is disappointing. Our models produce even less nickel and less energy than those computed with simpler and less accurate numerical schemes. In retrospect the reason for this finding is obvious. For a “healthy” explosion it is not sufficient to accelerate the burning front beyond what is predicted by previous numerical experiments, at least not in multi-dimensional models. In fact, more rapid *local* burning may under certain circumstances result in an expansion and cooling of the white dwarf *before* large amounts of nuclear fuel are consumed. Our centrally ignited models and the one with a single off-center blob are examples.

The question, therefore, remains whether or no our simulations rule out the deflagration scenario for typical Type Ia supernovae. Possible short-comings of the present numerical approach, such as the artificial symmetry assumption or the still insufficient numerical resolution, have already been mentioned. Here improvements will be possible with increasing computer power in the near future. It might also be worthwhile to investigate the behaviour of the simulations with varied parameter sets, e.g. for different chemical compositions or a slightly increased turbulent flame speed, since both of these quantities are not known exactly.

A second open question concerns our model of turbulent combustion. Here it is not clear at all, if one of our basic assumptions, namely that in the presence of reactions the turbulence spectrum is given by the Kolmogorov law remains valid. Although in the limit of very high turbulence intensity experi-

ments seem to support our hypothesis more work needs to be done. Also, significant burning is still possible at low densities in the so-called distributed regime, and even a transition to a detonation is not ruled out there (Niemeyer & Woosley, 1997).

Finally, white dwarfs at the onset of the explosion might look rather different from the ones we have used as initial conditions. URCA-neutrino emission and non stationary convection during the evolution just prior to the explosion have already been mentioned as likely sources of large uncertainties. Also, whether the star reaches the Chandrasekhar-mass by accretion or by merging with a companion will make a big difference. For example, rotation in some form may directly affect the propagation of the deflagration front. All these questions need to be investigated before we can safely dismiss the deflagration models.

*Acknowledgements.* This work was supported in part by the Deutsche Forschungsgemeinschaft under Grant Hi 534/3-1 and by DOE under contract No. B341495 at the University of Chicago. The computations were performed at the Rechenzentrum Garching on a Cray J90. The authors thank E. Bravo for many constructive suggestions which led to a significant improvement of this paper.

## References

- Abdel-Gayed R.G., Bradley D., Lawes M., 1987, Proc. R. Soc. Lond. A 414, 389
- Arnett W.D., Livne E., 1994, ApJ 427, 315
- Clement M.J., 1993, ApJ 406, 651
- Fryxell B.A., Müller E., Arnett W.D., 1989, MPA Preprint 449
- Hillebrandt W., Niemeyer J.C., 1997, In: Ruiz-Lapuente P., Canal R., Isern J. (eds.) *Thermonuclear Supernovae*. Kluwer Academic Publishers, Dordrecht, 337
- Iben I., Tutukov A.V., 1991, ApJ 370, 615
- Khokhlov A.M., 1991a, A&A 245, L25
- Khokhlov A.M., 1991b, A&A 245, 114
- Khokhlov A.M., 1991c, A&A 246, 383
- Khokhlov A.M., 1995, ApJ 449, 695
- Livne E., 1993, ApJ 406, L17
- Livne E., 1996, In: Ruiz-Lapuente P., Canal R., Isern J. (eds.) *Thermonuclear Supernovae*. Kluwer Academic Publishers, Dordrecht, 425
- Niemeyer J.C., 1995, *On the Propagation of Thermonuclear Flames in Type Ia Supernovae*. Ph.D. Thesis, Max-Planck-Institut für Astrophysik, Garching
- Niemeyer J.C., Hillebrandt W., 1995, ApJ 452, 769
- Niemeyer J.C., Hillebrandt W., Woosley S.E., 1996, ApJ 471, 903
- Niemeyer J.C., Woosley S.E., 1997, ApJ 475, 740
- Nomoto K., Thielemann F.K., Yokoi K., 1984, ApJ 286, 644
- Osher S., Sethian J.A., 1988, JCP 79, 12
- Reinecke M.A., Hillebrandt W., Niemeyer J.C., Klein R., 1999, A&A 347, 746
- Smiljanovski V., Moser V., Klein R., 1997, Comb. Theory and Modeling 1, 183
- Woosley S.E., 1990, In: Petschek A.G. (ed.) *Supernovae*. Berlin, Springer, 182
- Woosley S.E., Weaver T.A., 1994, ApJ 423, 371